BIOCHEMISTRY
including biophysical chemistry & molecular biology

Article

pubs.acs.org/biochemistry

Monomeric 14-3-3ζ Has a Chaperone-Like Activity and Is Stabilized by Phosphorylated HspB6

Nikolai N. Sluchanko,*[,†,‡] Natalya V. Artemova,[†] Maria V. Sudnitsyna,[‡] Irina V. Safenkova,[†] Alfred A. Antson,[§] Dmitrii I. Levitsky,[†] and Nikolai B. Gusev[‡]

[†]A. N. Bach Institute of Biochemistry, Russian Academy of Sciences, Leninsky Prospect 33, Moscow 119071, Russian Federation

[‡]Department of Biochemistry, School of Biology, Moscow State University, Lenin Hills 1, Building 12, Moscow 119234, Russian Federation

[§]York Structural Biology Laboratory, Department of Chemistry, University of York, York YO10 5YW, United Kingdom

Supporting Information

ABSTRACT: Members of the 14-3-3 eukaryotic protein family predominantly function as dimers. The dimeric form can be converted into monomers upon phosphorylation of Ser[58] located at the subunit interface. Monomers are less stable than dimers and have been considered to be either less active or even inactive during binding and regulation of phosphorylated client proteins. However, like dimers, monomers contain the phosphoserine-binding site and therefore can retain some functions of the dimeric 14-3-3. Furthermore, 14-3-3 monomers may possess additional functional roles owing to their exposed intersubunit surfaces. Previously we have found that the monomeric mutant of 14-3-3ζ (14-3-3ζ_m), like the wild type protein, is able to bind phosphorylated small heat shock protein HspB6 (pHspB6), which is involved in the regulation of smooth muscle contraction and cardioprotection. Here we report characterization of the 14-3-3ζ_m/pHspB6 complex by biophysical and biochemical techniques. We find that formation of the complex retards proteolytic degradation and increases thermal stability of the monomeric 14-3-3, indicating that interaction with phosphorylated targets could be a general mechanism of 14-3-3 monomers stabilization. Furthermore, by using myosin subfragment 1 (S1) as a model substrate we find that the monomer has significantly higher chaperone-like activity than either the dimeric 14-3-3ζ protein or even HspB6 itself. These observations indicate that 14-3-3ζ and possibly other 14-3-3 isoforms may have additional functional roles conducted by the monomeric state.

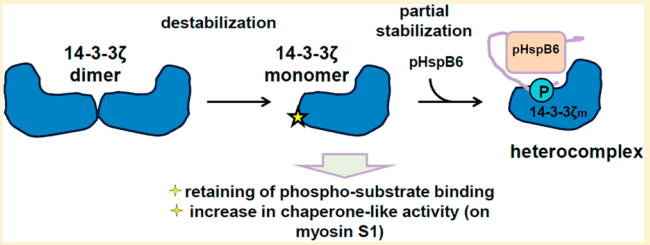

14-3-3s are well-known universal adapter proteins of small size (28−30 kDa), which are widely distributed among eukaryotes. These proteins participate in multiple cellular processes due to their ability to recognize over 300 partner proteins.[1] The partner proteins usually contain phosphorylated Ser/Thr within one of the three established consensus motifs.[2,3] It is thought that 14-3-3s act as homo- and/or heterodimers formed by different isoforms encoded by distinct genes.[4] The dimeric cup-like structure of the 14-3-3[5] is extremely stable. Stability of 14-3-3 was put into a basis of the popular "molecular anvil hypothesis", according to which the rigid 14-3-3 dimer can force structural rearrangements in some partner molecules, thereby regulating their activity and properties.[6] Binding of 14-3-3 can stabilize the structure of certain target proteins and prevent their dephosphorylation and/or degradation.[7,8] Indeed, phosphorylation followed by 14-3-3 binding plays an important role in regulation of apoptosis, cell division, signal transduction, ion-channels functioning, etc.[4] 14-3-3s bind diverse protein targets and can also prevent aggregation of certain model protein substrates.[9−11] This chaperone-like activity of 14-3-3 is not strictly dependent on target protein phosphorylation[9−11] and was suggested to play an important role in pathogenesis of certain neurodegenerative diseases.[12,13] It was proposed that the phosphopeptide binding and a chaperone-like action of 14-3-3 are functionally and structurally separated;[10] however, until now the exact regions responsible for chaperone-like activity of 14-3-3 have not been identified.

Until recently the dimeric form of 14-3-3 was considered to be crucial for most of its activities.[14] Phosphorylation of Ser[58] located at the dimer interface can regulate the dimeric state of 14-3-3,[15] and phosphomimicking mutation S58E induces partial dissociation of 14-3-3 dimers.[16] However, the presence and functional activity of 14-3-3 monomers remain questionable. It is known that a 14-3-3 dimer, having two binding sites, interacts with doubly phosphorylated peptides with 30-fold higher affinity than with singly phosphorylated peptides.[2] Therefore it appears that upon dissociation 14-3-3 will lose its ability to regulate partners that have more than one 14-3-3-binding site. Moreover, the dimeric state of 14-3-3 was proposed[16] and further demonstrated[17] to be essential for stability of 14-3-3 in vivo. However, 14-3-3 monomers participating in the 14-3-3

Received: May 23, 2012
Revised: July 1, 2012
Published: July 13, 2012

dx.doi.org/10.1021/bi300674e | *Biochemistry* 2012, 51, 6127−6138

homo- and heterodimer formation and accumulating upon phosphorylation of Ser[58] by a range of protein kinases[18] still possess phosphopeptide binding site and hypothetically can retain some functionality and even can acquire a new one. Intriguingly, the recently discovered alternatively spliced monomeric variant of human 14-3-3ε lacking the first 22 N-terminal residues was sufficient to protect HEK293 cells from UV-induced apoptosis by a yet unknown mechanism.[19]

Thus, despite an attractiveness of the hypothesis postulating instability of 14-3-3 monomers and their inability to interact with and to regulate their partners, the real situation appears to be more complex. Indeed, studies using artificial dimer-deficient mutants showed that the monomeric 14-3-3 can bind Raf kinase (but is unable to regulate its activity)[20] and interact with cytoplasmic part of the glycoprotein Ibα (GPIbα).[21] Using the *Drosophila* system, the monomeric form was shown to interact with and modulate activity of a slowpoke calcium-dependent potassium channel.[22] However, all these investigations were performed at a cellular level on dimer-deficient mutants of 14-3-3, which were not characterized structurally. Therefore, the question remained whether these mutant proteins were good model systems for in vitro and in vivo studies. Earlier we found that substitution of only three amino acids at the dimer interface of the human 14-3-3ζ (^{12}LAE^{14} → ^{12}QQR^{14}) leads to a complete dissociation of 14-3-3ζ without affecting its helical folding.[23] We also demonstrated that such monomeric mutant of 14-3-3ζ interacts with phosphorylated small heat shock protein HspB6 (Hsp20) with affinity comparable to (or even higher than) that of the wild type (WT) dimeric protein.[23]

In the present study we have characterized the interaction of the monomeric 14-3-3ζ mutant with phosphorylated HspB6 (pHspB6) by several biophysical and biochemical methods. We found that the 14-3-3ζ monomer can be significantly stabilized upon interaction with the phosphorylated target. We also compared the chaperone-like activities of the HspB6 and the wild type dimeric 14-3-3ζ with that of the monomeric 14-3-3ζ and demonstrated that the monomeric protein has the highest chaperone-like activity, effectively preventing a heat-induced aggregation of myosin subfragment 1 (S1).

EXPERIMENTAL PROCEDURES

Cloning, Protein Expression, and Purification. cDNA of the full-length wild type human 14-3-3ζ was cloned into pET23b vector using *NdeI* and *XhoI* restriction sites as described earlier.[16] The resulting plasmid was used for creation of the so-called WMW monomeric mutant form of 14-3-3 (here, 14-3-3ζ$_m$), carrying three amino acid replacements of ^{12}LAE^{14} by ^{12}QQR^{14}.[23] The WT human HspB6 (Hsp20) was also cloned into pET23b using *NdeI* and *XhoI* sites as described earlier.[24] Like 14-3-3ζ$_m$, S16D mutant of HspB6 was obtained by the site-directed mutagenesis as described earlier.[23,24] The integrity and correctness of all constructs were verified by DNA sequencing in Evrogen (Moscow, Russia, http://evrogen.ru/).

Corresponding plasmids were used to transform chemically competent *Escherichia coli* BL21(DE3)pLysS or Rosetta cells. Protein expression was induced by addition of 1 mM IPTG.[23] Protein purification included ammonium sulfate fractionation followed by anion-exchange chromatography using a High Trap Q column (Amersham Biosciences) and size-exclusion chromatography using a Superdex 200 column (Amersham Biosciences). Rabbit skeletal myosin subfragment 1 (S1) was prepared by chymotrypsinolysis of myosin filaments.[25] All proteins were homogeneous according to the SDS−PAGE.[26] Protein concentrations were measured by absorbance at 280 nm.[23]

Phosphorylation of HspB6. HspB6 was phosphorylated by catalytic subunit of a recombinant mouse protein kinase A (PKA).[27] The reaction was started by addition of PKA and lasted for 1 h at 37 °C. EDTA was added up to the final concentration of 10 mM to stop the reaction. The 100 μL aliquots of reaction mixture were frozen and stored at −20 °C. This procedure led to incorporation of approximately one mole of phosphate per mole of HspB6 and was accompanied by an increase in the electrophoretic mobility of HspB6 on the native gel electrophoresis as observed earlier.[27]

Asymmetrical Flow Field-Flow Fractionation Coupled with Multiangle Laser Light Scattering (AF4-MALLS). AF4 was performed using an Agilent autosampler and pump connected to a Wyatt Eclipse 3+ Separation System (Wyatt Technology Corp., USA). Detection included an Agilent UV detector (Agilent Technologies Inc., USA) as well as Dawn HELEOS II online multiangle laser light scattering (MALLS) detector and OptilabT-Rex differential refractive index (RI) detector (both Wyatt Technology). Separations were performed using a 5-kDa MW cutoff regenerated cellulose membrane (Microdyn-Nadir GmbH, Germany) in the 275-mm channel with 350-μm thick spacer. The samples (0.5−2 mg/mL) were prepared in AF4 buffer (20 mM Tris-HCl, pH 7.5, 150 mM NaCl, 2 mM $MgCl_2$, 15 mM ME) and loaded in 40 μL volume (20−80 μg of protein per load). The collected light scattering data were fitted to the Zimm formalism using Astra v5.3.4 software (Wyatt Technology) for calculation of weight-averaged molar mass.

Limited Chymotrypsinolysis. Chymotrypsinolysis was performed in buffer C (20 mM Tris/acetate, pH 7.5, 10 mM NaCl, 2 mM DTT) at 37 °C and the weight ratio TLCK-treated chymotrypsin/substrate equal to 1:1000−1:5000. Isolated unphosphorylated or phosphorylated HspB6 (pHspB6) (0.52 mg/mL or 29 μM per monomer), isolated 14-3-3ζ WT or 14-3-3ζ$_m$ (0.81 mg/mL or 29 μM per monomer), or the mixtures of unphosphorylated/phosphorylated HspB6 with either 14-3-3ζ WT or 14-3-3ζ$_m$ were incubated with protease for different time intervals; each reaction was stopped by addition of the SDS-sample buffer containing PMSF up to the final concentration of 2 mM. The samples were boiled and analyzed by SDS−PAGE on 15% polyacrylamide gels. Quantitative densitometry was performed using ImageJ 1.45s software. To determine the nature of proteolytic peptides samples were collected after 60 min incubation (weight ratio protease/substrate of 1:1000), each reaction was stopped by addition of 2 mM PMSF. Desalted samples were analyzed using MALDI TOF/TOF ultrafleXtreme mass-spectrometer (Bruker, Germany) and using the massXpert software.[28]

To analyze the effect of phosphate on 14-3-3 chymotrypsinolysis, we used two buffers with identical ionic strength, but different composition, namely, 20 mM Tris/HCl buffer (pH 7.5), containing 115 mM NaCl and 2 mM DTT or 50 mM Na-phosphate buffer (pH 7.5), containing 2 mM DTT. 14-3-3ζ$_m$ (0.81 mg/mL) or BSA (0.5 mg/mL) as a control were incubated for 25 min at 37 °C in these buffers and then subjected to chymotrypsinolysis. The weight ratio TLCK-chymotrypsin/substrate was 1:1000 in the case of 14-3-3 and 1:200 in the case of BSA. The protein composition of the samples was analyzed by SDS−PAGE followed by quantitative densitometry.

CD Spectroscopy. Far-UV CD spectra of HspB6 or pHspB6 (0.4 mg/mL), 14-3-3ζ WT, and 14-3-3ζ_m (0.6 mg/mL) were recorded at 20 °C in buffer CD (8 mM HEPES/Na (pH 7.3), 25 mM NaCl, 0.25 mM $MgCl_2$, 2 mM DTT). All spectra were recorded in the range of 190−260 nm at a rate of 0.5 nm/min in 0.2 mm cell on a Chirascan circular dichroism spectrometer (Applied Photophysics).

To determine the thermal stability of proteins, 14-3-3ζ_m alone (0.6 mg/mL or 22 μM per monomer) or its equimolar mixture with phosphorylated or unphosphorylated HspB6 (22 μM) was incubated in buffer CD for 30 min at 37 °C. Samples were further heated with a rate of 1 °C/min in the range of 20−70 °C with simultaneous registration of ellipticity at 222 nm. The data were transformed into dependence of the fraction of folded protein $[(\Theta_{T,°C} - \Theta_{70°C})/(\Theta_{20°C} - \Theta_{70°C})*100\%]$ on temperature (T, °C).[29] By plotting $d[\Theta_{222}]/dT$[29] against temperature, we were able to determine maxima corresponding to the thermal transition of isolated proteins or their mixture.

Fluorescence Measurements. Intrinsic Trp fluorescence of HspB6 and pHspB6 (0.055−0.16 mg/mL or 3−9 μM per monomer) was recorded at 25 °C in buffer F (20 mM HEPES/Na, pH 7.3, 100 mM NaCl, 4 mM $MgCl_2$, 15 mM ME). Fluorescence was excited at 297 nm and recorded in the range of 310−400 nm (slits width 5 nm) on a Cary Eclipse spectrofluorometer (Varian Inc.).

Fluorescence spectroscopy was also used for registration of temperature-induced changes in protein structure. 14-3-3ζ_m alone (0.2 mg/mL or 7 μM per monomer) or its mixture with phosphorylated or unphosphorylated HspB6 (7 μM per monomer) was incubated in buffer F for 20−30 min at 37 °C. Fluorescence was excited at 297 nm (slit width 5 nm) and recorded at 320 or 365 nm (slit width 2.5 nm). The protein samples were heated in the range of 15−80 °C with the rate of 1 °C/min in automatic Peltier Multicell Holder of Cary Eclipse spectrofluorometer (Varian Inc.) and cooled back with the same rate. For determination of the half-transition temperatures, we plotted completeness of transition determined by the method of Permyakov and Burstein[30] against temperature.

To investigate protein aggregation induced by elevated temperatures, we also monitored light scattering of the samples during its heating from 15 up to 80 °C with 1 °C/min rate. The light scattering was recorded by enlightening the sample at 350 nm and measuring scattering at 355 nm (slits width 5 nm). All data were corrected for retardation of the temperature inside the cell, compared to the cell holder, during heating.

Differential Scanning Calorimetry (DSC). DSC was used to analyze thermal denaturation of 14-3-3ζ WT, its S58E and S58E/S184E/T232E mutants mimicking naturally occurring phosphorylation,[27] and also for estimation of the thermal stability of 14-3-3ζ_m and HspB6. Protein samples containing 14-3-3ζ WT or 14-3-3ζ_m (0.9 mg/mL or 32 μM per monomer), phosphorylated or unphosphorylated HspB6 (0.9 mg/mL or 50 μM per monomer), or the mixture of 14-3-3ζ_m with either HspB6 or pHspB6 (32 μM of 14-3-3 and 50 μM of HspB6) in buffer DSC (30 mM HEPES/Na buffer, pH 7.3, containing 100 mM NaCl, 1 mM $MgCl_2$) were heated at a constant rate of 1 °C/min from 5° up to 85 °C on a DASM-4 M differential scanning calorimeter (Institute for Biological Instrumentation, Pushchino, Russia). The thermal unfolding of all proteins studied was fully irreversible as judged from comparison with a second heating of the same sample. Calorimetric curves were corrected for instrumental background as described earlier[31] and transition temperature (T_m) was determined from the maximum of the thermal transition.

Thermal Aggregation of Myosin Subfragment 1 (S1). Aggregation of isolated S1 (0.46 mg/mL) or its aggregation in the presence of 14-3-3ζ_m, 14-3-3ζ WT, or HspB6 at different S1/chaperone weight ratios (1:0.1−1:1) was monitored by measuring an apparent absorbance at 360 nm at 43 °C in 20 mM HEPES/Na buffer (pH 7.0), containing 115 mM NaCl and 4 mM DTT. Under these conditions aggregation of S1 started after 20−30 min incubation at 43 °C. All measurements were performed on a Cary 100 UV−visible spectrophotometer (Varian Inc.) equipped with a Biomelt multicell holder.

RESULTS

14-3-3ζ_m Interacts with Phosphorylated HspB6, but not with Its Phosphomimicking Mutant (S16D) or Unphosphorylated HspB6. To investigate the interaction between 14-3-3ζ_m and HspB6 and to estimate molecular mass and stoichiometry of the complex, we used asymmetric flow field-flow fractionation (AF4) coupled with multiangle laser light scattering (MALLS) detector and refractometer. In this system the smaller particles were focused and eluted first followed by particles of larger size. This system provides information about homogeneity and molecular masses of molecules that are separated by size.

14-3-3ζ_m eluted as a narrow peak (Figure 1A; curve 1) corresponding to monodisperse particles with a mass of 27.8 ± 0.3 kDa and polydispersity index (PDI) of 1.01 ± 0.01 (Supplemental Figure S1). These values are in good agreement with our previous data.[23] HspB6 was eluted as a broad peak with a maximum at 14.5−15 min (Figure 1A; curve 2). However, HspB6 was also almost monodisperse (Figure S1) with the PDI of 1.02 ± 0.08 and was likely presented by dimers (M_w = 33.9 kDa ± 0.9 kDa), having different conformation in solution. When 14-3-3ζ_m was mixed with phosphomimicking mutant of HspB6 (S16D) or with unphosphorylated HspB6 the elution profile was indistinguishable from the algebraic sum of the profiles corresponding to isolated proteins (Figure 1A; compare curves 1 + 2 and 3). This means that 14-3-3ζ_m does not interact with either phosphomimicking mutant of HspB6 (S16D) or with unphosphorylated HspB6. However the elution profile changed significantly when HspB6 phosphorylated by PKA was mixed with 14-3-3ζ_m (Figure 1A, curves 4 and 5). In this case the elution profile was substantially different from the algebraic sum of elution profiles of isolated 14-3-3ζ and HspB6 (Figure 1A; compare curves 4 and 5 with curve 1 + 2). When the mixture subjected to fractionation contained an excess of 14-3-3ζ_m, we detected two peaks, apparently corresponding to free 14-3-3ζ_m and to the complex of 14-3-3ζ_m with phosphorylated HspB6 (Figure 1A; curve 4). In the case of an equimolar mixture of 14-3-3ζ_m and phosphorylated HspB6, we observed only one peak corresponding to the complex formed by these two proteins (Figure 1A; curve 5). Moreover, the fractions from this peak contained equal quantities of both proteins (Figure 1B), again indicating formation of the complex in a 1:1 molar ratio. This conclusion was finally confirmed by the mass distribution of the particles eluted in the peak corresponding to this complex (Figure S1). The complex formed by the two proteins was almost monodisperse (PDI = 1.01 ± 0.02) with a molecular mass of 45.0 ± 1.0 kDa that correlates well with the sum of the calculated masses of 14-3-3ζ (27.75 kDa) and HspB6 (17.14 kDa) monomers.

dx.doi.org/10.1021/bi300674e | Biochemistry 2012, 51, 6127−6138

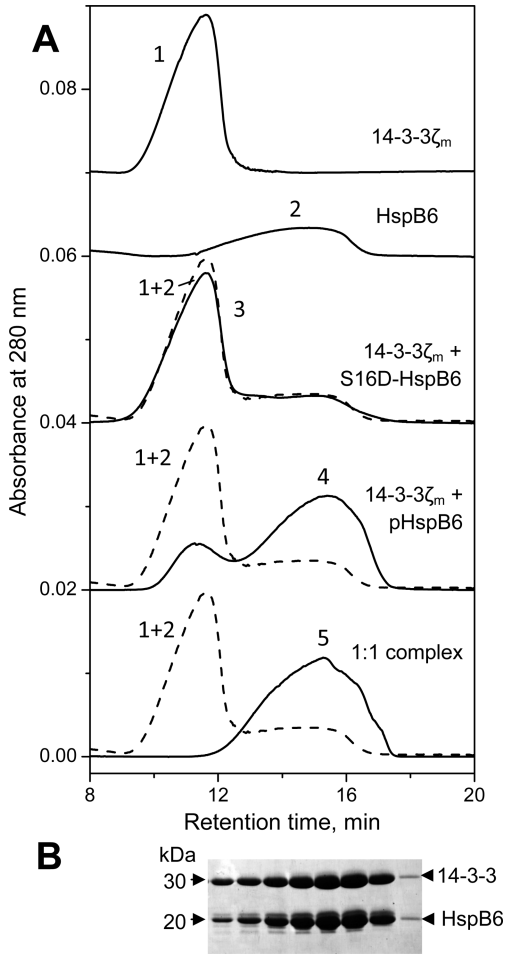

Figure 1. Interaction of 14-3-3ζ_m with HspB6 analyzed by asymmetric flow field flow fractionation. (A) Elution profiles of 14-3-3ζ_m (47 μM; curve 1), pHspB6 (33 μM; curve 2), the mixture of 14-3-3ζ_m with S16D mutant of HspB6 (47 μM of 14-3-3ζ_m and 33 μM of HspB6; curve 3), the mixture of 14-3-3ζ_m with pHspB6 (47 μM of 14-3-3ζ_m and 33 μM of HspB6; curve 4), and equimolar complex of 14-3-3ζ_m with pHspB6 (33 μM of each respective to monomers; curve 5) obtained under conditions described in Experimental Procedures. For comparison, the algebraic sum of 14-3-3ζ_m and HspB6 elution profiles is also added to the plot (dashed curve 1 + 2). (B) SDS gel electrophoresis of fractions from the peak of the complex formed by pHspB6 and 14-3-3ζ_m. Typical result is shown. The positions of molecular mass standards (in kDa), 14-3-3 and HspB6 are indicated by arrows.

Thus, the monomeric mutant of 14-3-3ζ has the same selectivity and specificity as the dimeric 14-3-3ζ. It is unable to bind unphosphorylated HspB6 or its S16D mutant and forms a tight complex with phosphorylated HspB6. Interaction with 14-3-3ζ_m presumably induces dissociation of the HspB6 dimer as the stoichiometry of the heterocomplex formed is close to 1:1.

Phosphorylated HspB6 Makes 14-3-3ζ_m Less Susceptible to Proteolysis. It is possible that tight interaction between 14-3-3ζ_m and phosphorylated HspB6 can affect structure of individual proteins within the complex. In order to analyze the effect of phosphorylated HspB6 on 14-3-3ζ_m, we used several biophysical and biochemical methods.

We first analyzed the effect of HspB6 on limited proteolysis of 14-3-3ζ. Trypsinolysis of 14-3-3ζ leads to accumulation of a major comparably stable peptide of ~20 kDa,[16,23] which can interfere with the band of intact HspB6 having the same apparent molecular weight on SDS–PAGE. Therefore, we used chymotrypsin which produces only a minor 14-3-3-derived peptide with an apparent molecular mass ~20 kDa and two other major peptides with slightly lower (~17–18 kDa) and significantly higher (~24 kDa) apparent molecular masses as compared with HspB6 (Figure 2A, 14-3-3ζ_m).

In good agreement with the earlier data,[23] we found that 14-3-3ζ_m is more susceptible to proteolysis than the wild type protein. For instance, even 90 min incubation of the wild type

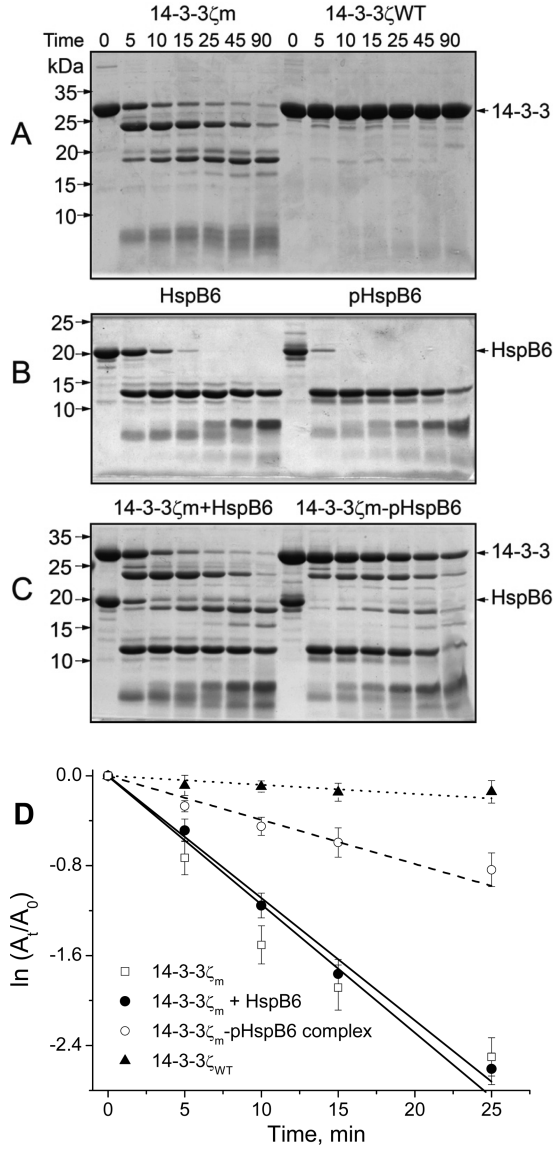

Figure 2. Limited chymotrypsinolysis of 14-3-3ζ (A), HspB6 (B), and their mixture (C). The samples, containing 14-3-3ζ (0.81 mg/mL), HspB6 (0.52 mg/mL), or both proteins (indicated above each gel) were incubated at 37 °C in the presence of TLCK-chymotrypsin at a weight ratio protease/substrate of 1:1000 and analyzed by SDS–PAGE. Time of incubation (in min) is indicated on the top of each lane. Positions of molecular mass standards (in kDa), and positions of 14-3-3 and HspB6 are indicated by arrows. (D) Kinetics of the 14-3-3 band degradation during chymotrypsinolysis of isolated 14-3-3ζ_m (open squares), isolated 14-3-3ζ WT (filled triangles), or of the mixture of 14-3-3ζ_m with either unphosphorylated (filled squares) or phosphorylated HspB6 (open circles). A_t represents 14-3-3 band intensity at the time point t and A_0 represents initial intensity.

dx.doi.org/10.1021/bi300674e | *Biochemistry* 2012, 51, 6127–6138

protein with chymotrypsin was not accompanied by a significant decrease in the intensity of the band corresponding to the intact 14-3-3 (Figure 2A), whereas even a short 10 min incubation with chymotrypsin leads to significant disappearance of the 14-3-3ζ_m band (Figure 2A). Peptide patterns observed after chymotrypsinolysis of both unphosphorylated and phosphorylated HspB6 were very similar (Figure 2B); however, the rate of proteolysis of phosphorylated HspB6 was noticeably higher than that of the unphosphorylated protein (Figure 2B). If the mixture of 14-3-3ζ_m and HspB6 was subjected to proteolysis, the pattern of accumulated peptides was identical to the sum of patterns observed for two isolated proteins. Addition of unphosphorylated HspB6 had no effect on the rate of 14-3-3ζ_m chymotrypsinolysis (Figure 2C, left). On the contrary, when the 14-3-3ζ_m–pHspB6 complex was subjected to proteolysis, the rate of 14-3-3ζ_m degradation and concomitant accumulation of 14-3-3-derived peptides of ~24 and ~17 kDa was significantly decreased (compare left and right panels of Figure 2C,D). The data presented indicate that interacting with 14-3-3ζ_m phosphorylated (but not unphosphorylated) HspB6 stabilizes the 14-3-3ζ_m structure. At the same time the complex formation does not affect the rate of pHspB6 proteolysis and as before phosphorylated HspB6 was less stable than its unphosphorylated counterpart (compare left and right panels on Figure 2B,C). Since retardation of 14-3-3ζ_m proteolysis was observed even after complete degradation of intact pHspB6, we can suppose that stabilization of 14-3-3ζ_m is induced by short peptides of HspB6 containing Ser^{16} in consensus sequence recognized by 14-3-3.[9,32]

Which of pHspB6 Peptides Stabilize 14-3-3ζ_m? To identify specific peptides of phosphorylated HspB6 that could stabilize 14-3-3ζ_m, we used MALDI/TOF mass spectrometry and analyzed the composition of chymotryptic peptides obtained after proteolysis of 14-3-3ζ_m alone or in the presence of phosphorylated or unphosphorylated HspB6 (data not shown). The main and the largest peptide of HspB6 also visible on the gels on Figure 2B,C had the molecular mass of 11450/11531 Da and corresponded to singly phosphorylated (~80 Da) C-terminal peptide $HspB6_{a.a.54–160}$. This peptide of HspB6 contains a rather stable α-Crystallin domain.[33] The next peptide having a molecular mass of 7180/7259 Da corresponded to a shorter $HspB6_{a.a.54–117}$ fragment also containing a single phosphorylated site (~80 Da). Mass prediction by massXpert[28] indicated that both phosphorylated peptides remaining resistant to proteolysis derive from the C-terminal part of the molecule and contain Ser^{59}. This site is only weakly phosphorylated by PKA and is not phosphorylated by PKG,[34] and the primary structure at Ser^{59} (RAPS^{59}VA) differs from the consensus motifs recognized by 14-3-3.[2] Moreover, prolonged incubation with chymotrypsin (90 min) results in practically complete degradation of 11450/11531 peptide of phosphorylated HspB6 with a significant portion of 14-3-3 remaining uncleaved (Figure 2C, right). At the same time even after long incubation (90 min), a rather large portion of 11450/11531 peptide of unphosphorylated HspB6 remained uncleaved, whereas the band of 14-3-3 was completely vanished (Figure 2C, left). Therefore, it seems very unlikely that the peptides containing weakly phosphorylated Ser^{59} bind to and stabilize 14-3-3ζ_m. Thus, the major peptides of HspB6 visible on Figure 2B,C cannot account for 14-3-3ζ_m stabilization.

It is reasonable to suppose that the fragment of HspB6 containing the major site phosphorylated by PKA, that is, Ser^{16}, is responsible for 14-3-3ζ_m stabilization. However, secondary structure predictions (Figure S2) indicate that the N-terminus of HspB6 is unstructured and therefore highly susceptible to proteolysis. In addition, this part of the molecule contains many aromatic and hydrophobic residues (e.g., Trp^{11}, Phe^{29}, Phe^{33}, Tyr^{53}, Tyr^{54} shown on Figure S2) that could serve as potential cleavage sites for chymotrypsin. Since the N-terminal part of HspB6 is accessible to chymotrypsinolysis, even short incubation with protease is accompanied by formation of very short peptides which cannot be unequivocally detected on SDS–PAGE and determined by mass-spectroscopy. Utilization of trypsin will lead to the same situation as the flexible N-terminus of HspB6 contains many potential sites for trypsin cleavage (e.g., Arg^{13}, Arg^{14}, Arg^{27}, Arg^{32}, Arg^{56}, Figure S2), and this will again lead to accumulation of short peptides. These features hamper unequivocal determination of stabilizing peptide of HspB6.

The minimal 14-3-3-binding fragment of pHspB6, RRApS^{16}APL, does not contain potential sites for chymotrypsinolysis and would remain intact even under exhaustive digestion. We suppose that all peptides derived from the N-terminus of phosphorylated HspB6 and containing RRApS^{16}APL fragment are able to interact with 14-3-3ζ_m and retard its proteolysis. If this suggestion is correct, the ligand-bound state of 14-3-3ζ_m is more stable to limited chymotrypsinolysis than its form devoid of target peptides/proteins.

Effect of Phosphate on Chymotrypsinolysis of 14-3-3ζ_m. Inorganic phosphate can affect interaction of 14-3-3 with its ligands.[35,36] We supposed that phosphate somehow imitates interaction of 14-3-3 with its ligands and therefore can affect chymotrypsinolysis of 14-3-3ζ_m. To check this suggestion we performed 14-3-3ζ_m chymotrypsinolysis in two buffers that had the same ionic strength and pH but differed in chemical composition, that is, 20 mM Tris/HCl pH 7.5 containing 115 mM NaCl (Figure 3A, left) and 50 mM Na/phosphate pH 7.5 (Figure 3A, right). We varied ionic strength and phosphate concentration; however, in all cases the presence of phosphate led to a significantly reduced rate of 14-3-3ζ_m proteolysis (Figure 3A,C). This effect was specific to 14-3-3ζ_m and could not be explained by lower protease activity in phosphate buffer. Indeed, the rate of chymotrypsinolysis of BSA was even slightly higher in phosphate than in Tris buffer (Figure 3B,C). These results agree with earlier observations indicating that phosphate might activate chymotrypsin.[37] However, phosphate inhibited chymotrypsinolysis of 14-3-3ζ_m supporting our hypothesis that binding of small molecules mimicking substrate makes 14-3-3ζ_m more stable. At the same time, this also means that it is desirable to avoid utilization of phosphate buffers in any studies analyzing interaction of 14-3-3 with phosphorylated partners since phosphate can inhibit this interaction.

Stabilization of 14-3-3ζ_m by pHspB6 Determined by Far-UV CD Spectroscopy. It has been shown that the monomeric mutant of 14-3-3ζ possesses the same α-helical structure as the WT dimeric protein but is less thermostable.[23] We supposed that phosphorylated HspB6 will affect not only stability to proteolysis but also thermal stability of 14-3-3ζ_m. We used far-UV CD spectroscopy to monitor the changes in the secondary structure of 14-3-3ζ_m upon heating. Isolated HspB6 is enriched in β-structure[33] and has a CD spectrum of low amplitude with a negative maximum at ~208 nm (see Figure 4A inset). Phosphorylation of HspB6 by PKA slightly decreased the amplitude of its CD spectrum (data not shown). In any case the amplitudes in the CD spectra of HspB6 or pHspB6 were very small in comparison with the α-helical 14-3-

dx.doi.org/10.1021/bi300674e | Biochemistry 2012, 51, 6127–6138

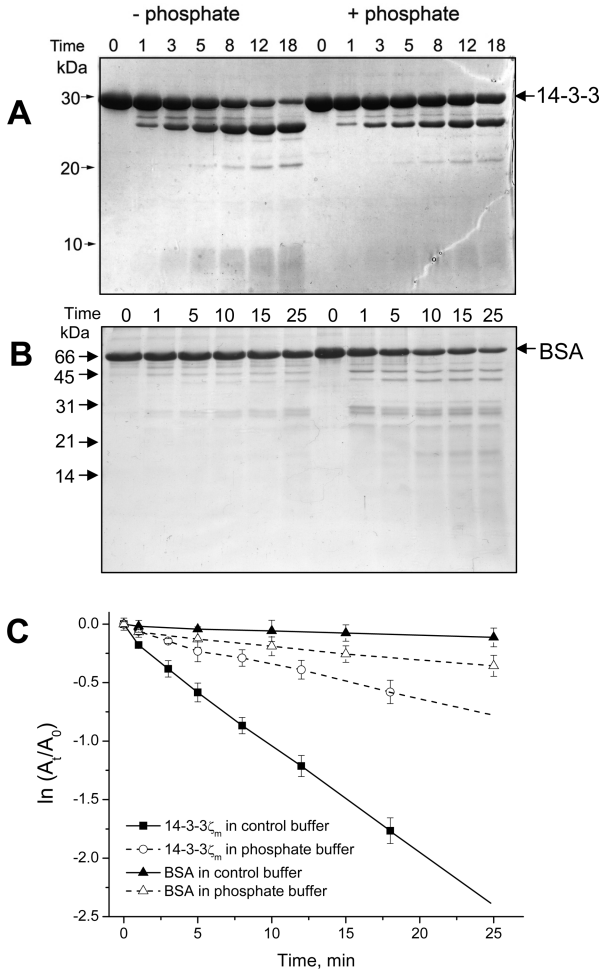

Figure 3. Effect of phosphate on the limited chymotrypsinolysis of 14-3-3ζ_m. (A, B) 14-3-3ζ_m (0.81 mg/mL) or BSA (0.5 mg/mL) in two buffers differing only by the presence or absence of phosphate was incubated at 37 °C with chymotrypsin at a weight ratio protease/substrate equal to 1:1000 (14-3-3ζ_m) or 1:200 (BSA) for different times (indicated above each lane in min). Protein composition of the samples was analyzed by SDS−PAGE. Molecular mass standards (in kDa) and positions of 14-3-3 and BSA are indicated by arrows. (C) Kinetics of the 14-3-3ζ_m or BSA band degradation determined by densitometry of the gels presented on panels A and B. A_t represents the intensity of the band at the time point t and A_0 represents initial intensity.

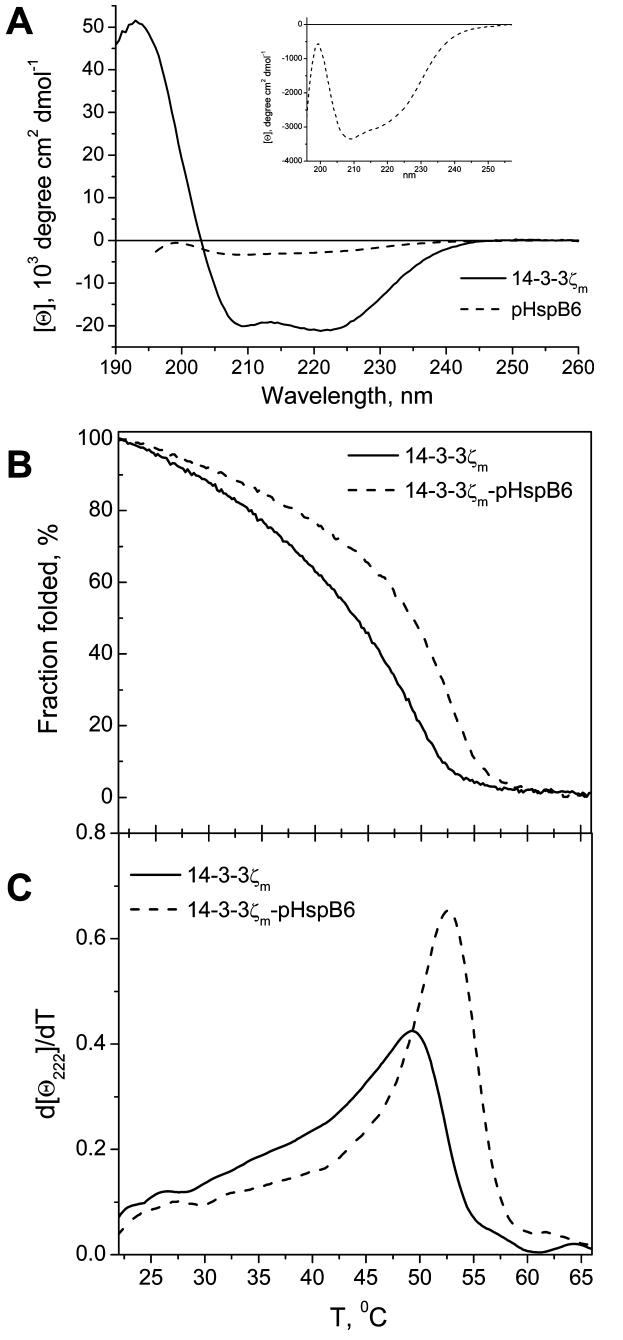

Figure 4. Investigation of the thermal stability of 14-3-3ζ_m by means of far-UV CD spectroscopy. (A) Far-UV CD spectra of 14-3-3ζ_m (0.6 mg/mL; solid line) and HspB6 (0.4 mg/mL; dashed line − main figure and inset). (B) Dependence of fraction of folded 14-3-3ζ_m alone (solid line) or in the complex with pHspB6 (dashed line) on temperature. The samples were preincubated for 30 min at 37 °C and heated from 20 to 70 °C at a constant rate of 1 °C/min on Chirascan dichroism spectrometer (Applied Biophysics). (C) The rate of 14-3-3ζ_m unfolding obtained by differentiating the curves presented on panel B. The temperatures characterizing the maximal unfolding rate of 14-3-3ζ_m with or without pHspB6 are presented in Table 1.

3 protein that has a pronounced negative maximum at 222 nm (Figure 4A). Therefore, by measuring ellipticity at 222 nm (Θ_{222}), we were able to follow temperature-induced changes in helicity of 14-3-3ζ_m independent of the presence of HspB6 in the sample.

Upon heating the fraction of folded 14-3-3ζ_m was gradually decreased and the protein became completely unfolded at ∼60 °C (Figure 4B,C). Addition of pHspB6 induced decrease in the unfolding rate of 14-3-3ζ_m (at temperatures below ∼47 °C) and increased cooperativity of the transition at the maximal unfolding rate (Figure 4B,C). The maximal rate of unfolding of isolated 14-3-3ζ_m was observed at 49.5 ± 0.3 °C, whereas in the presence of phosphorylated HspB6 the maximal rate of 14-3-3ζ_m unfolding was detected at 53.0 ± 0.1 °C (Figure 4C, Table 1). Thus, interaction with pHspB6 increases thermal stability of 14-3-3ζ_m measured by CD spectroscopy.

Estimation of Thermal Stability of 14-3-3ζ_m−pHspB6 Complex by Trp Fluorescence. Fluorescence spectroscopy was also used for analysis of the effect of pHspB6 on thermal stability of 14-3-3ζ_m. Trp[59] has been shown to determine the intrinsic fluorescence of 14-3-3ζ.[35] This tryptophan residue is located in the vicinity to the ligand-binding groove of 14-3-3,

dx.doi.org/10.1021/bi300674e | Biochemistry 2012, 51, 6127−6138

Table 1. Effect of pHspB6 on Thermal Stability of 14-3-3ζ_m[a]

sample	characteristic temperatures obtained by different methods, °C		
	CD spectroscopy	data of intrinsic fluorescence	DSC
14-3-3ζ_m	49.5 ± 0.3	51.1 ± 0.2	51.1 ± 0.1
14-3-3ζ_m in complex with pHspB6	53.0 ± 0.1	53.3 ± 0.1	53.9 ± 0.1

[a]All values represent mean values with standard errors.

and therefore its fluorescence can be successfully used for following interaction of 14-3-3 with its targets.

The only tryptophan residue of HspB6 (Trp^{11}) is located at the N-terminus very close to the 14-3-3-binding motif (see Figure S2). As already mentioned, theoretical predictions indicate that the N-terminus of HspB6 is very flexible and predominantly unordered. If these predictions are correct, Trp^{11} will be exposed to the solvent and will have fluorescence spectrum characteristic to Trp residues contacting with solvent and belonging to the so-called class II of Trp in proteins according to the classification of Burstein et al.[38] Indeed, normalized fluorescence spectrum of HspB6 completely coincides with the spectrum of class II Trp residues, and phosphorylation of HspB6 by PKA does not change its fluorescence (Figure S3, panel A). These data complement our conclusions about flexibility and unstructured nature of the N-terminus of HspB6.

Our data indicated that heating up to ~60 °C does not dramatically affect Trp fluorescence of HspB6 (Figure S3, panel B), and therefore the presence of HspB6 will not interfere with 14-3-3s Trp fluorescence at least at temperatures below 60 °C. We followed the thermally induced changes in the 14-3-3ζ_m fluorescence in the absence or presence of phosphorylated HspB6 and determined corresponding half-transition temperatures. Half-transition of isolated 14-3-3ζ_m occurred at 51.1 ± 0.2 °C (Figure S4, Table 1) in good agreement with our earlier published data.[23] Addition of phosphorylated HspB6 induced increase of half-transition temperature which became equal to 53.3 ± 0.1 °C (Figure S4, Table 1). Thus, both the data of CD and fluorescence spectroscopy indicate that binding of phosphorylated HspB6 increases thermal stability of 14-3-3ζ_m (Figure 4B,C, S4).

Stabilization of 14-3-3ζ_m by pHspB6 Determined by Differential Scanning Calorimetry (DSC). For more detailed analysis of the thermal unfolding of 14-3-3ζ_m in its complex with pHspB6, we applied differential scanning calorimetry (DSC), that is, the method commonly employed to study protein unfolding[39] and protein−protein interaction.[40] However, prior to DSC studies on the 14-3-3ζ_m−pHspB6 complex, it was necessary to analyze thermal unfolding of isolated protein partners.

Figure 5A shows that the monomeric mutant of 14-3-3ζ is much less thermostable than its dimeric counterpart. The thermal transition of 14-3-3ζ_m was observed at 51.1 °C, that is, at the temperature more than 10 °C less than the corresponding transition of the 14-3-3ζ WT (T_m = 61.8 °C). Interestingly, similar low temperature transitions (at 49.0−51.5 °C) were also observed on the DSC profile of 14-3-3ζ with S58E mutation mimicking phosphorylation of 14-3-3ζ occurring in vivo (Figure S5). This mutation, however, induced only partial dissociation of 14-3-3 dimers.[16,23] Therefore, on these thermograms we observed two peaks, presumably corresponding to 14-3-3 monomer (the low temperature peak) and dimer (the high temperature peak on Figure S5). Thermal unfolding of 14-3-3ζ_m was fully irreversible as it was accompanied by aggregation of the protein (Figure 6; curve 1).

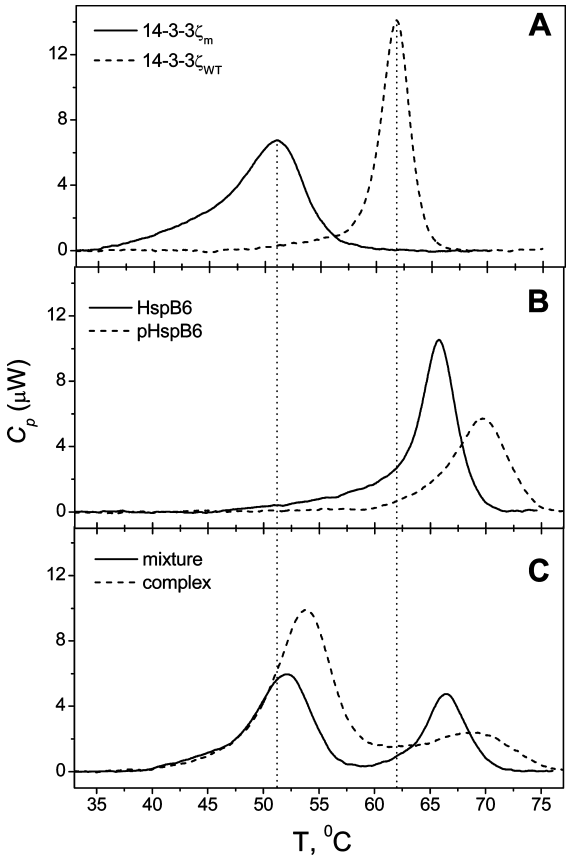

Figure 5. Thermal stability of 14-3-3ζ_m and HspB6 studied by DSC. The samples containing 14-3-3ζ_m (A; solid line) or 14-3-3ζ WT (A; dashed line) alone (0.9 mg/mL or 33 μM per monomer), HspB6 (B; solid line) or pHspB6 (B; dashed line) alone (0.9 mg/mL or 50 μM per monomer), or the mixture of 14-3-3ζ_m with HspB6 (C; solid line) or pHspB6 (C; dashed line) were heated from 5 to 80 °C at a rate of 1 °C/min on a DASM-4 M differential scanning calorimeter and the excess heat capacity (C_p) was measured during the heating. The initial curves were processed as described previously.[42] The transition temperatures (T_m) for proteins determined as maxima of the peaks on thermograms are presented in Table 1.

Figure 5B represents the DSC profiles for HspB6 and pHspB6. It is clearly seen that phosphorylation of HspB6 significantly increases the thermal stability of the protein by shifting its thermal transition by almost 4 °C toward a higher temperature, from 65.8 to 69.7 °C. It should be noted that the thermal denaturation of HspB6 was fully irreversible as no cooperative transitions were observed during reheating of the samples. In this respect, HspB6 is quite different from the other members of the sHsp family (αB-Crystallin (HspB5), HspB1, HspB8) whose thermal denaturation studied by DSC was completely reversible.[25,41,42] The irreversible nature of thermal denaturation of HspB6 seems to be due to its temperature-induced aggregation (Figure 6; curve 2), which also is not characteristic for the other members of the sHsp family.[25,43] It is noteworthy that phosphorylation of HspB6 not only makes it more thermostable (Figure 5B), but also dramatically reduces its aggregation measured by light scattering (Figure 6; curve 3).

dx.doi.org/10.1021/bi300674e | Biochemistry 2012, 51, 6127−6138

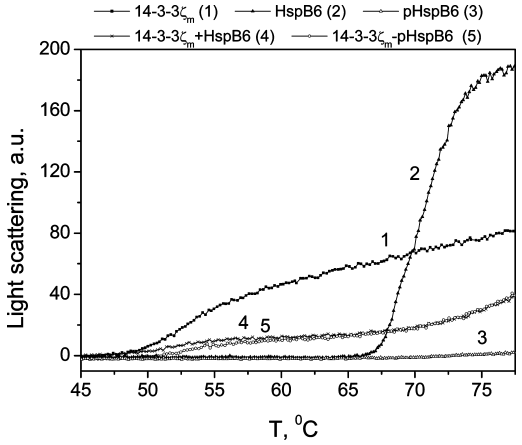

Figure 6. Aggregation of 14-3-3ζ_m and HspB6 measured by light scattering. The samples, containing 14-3-3ζ_m (10 μM per monomer; curve 1), or HspB6 (10 μM per monomer; curve 2), pHspB6 (10 μM per monomer; curve 3), or the mixture of 14-3-3ζ_m with HspB6 (curve 4) or pHspB6 (curve 5) were heated from 15 to 80 °C at a rate of 1 °C/min and the light scattering was simultaneously measured on a Cary Eclipse spectrofluorometer as described in Experimental Procedures.

DSC profiles obtained for 14-3-3ζ_m in the presence of either HspB6 or pHspB6 are represented on Figure 5C. In accordance with our earlier published data[23] and the data presented above (Figure 1), the monomeric 14-3-3ζ can interact only with phosphorylated HspB6, but not with unphosphorylated HspB6 or its S16D mutant. DSC profile of the mixture of 14-3-3ζ_m with ~1.5 molar excess of unphosphorylated HspB6 demonstrates two peaks roughly corresponding to the peaks of isolated proteins (Figure 5C; solid line). However, the peak of 14-3-3ζ_m became slightly shifted toward higher temperature and the area under the HspB6 thermal transition was significantly (by ~60%) decreased (Figure 5; compare solid lines on panel C and B). The above-mentioned minimal changes of thermogram can be due to the interaction of unphosphorylated HspB6 (acting as chaperone) with 14-3-3ζ_m which becomes unfolded in the course of heating. In favor of this assumption, the light scattering data show that HspB6 and 14-3-3ζ_m mutually prevent temperature-induced aggregation of each other (Figure 6, compare curves 1, 2, and 4).

Phosphorylated HspB6 induces much larger changes in thermogram of 14-3-3ζ_m. For instance, thermal transition of 14-3-3ζ_m is shifted by ~3 °C toward higher temperature (T_m increases from 51.1 to 53.9 °C, Table 1), and the area under this transition is significantly increased (by ~80% in comparison with that in the case of unphosphorylated HspB6) (Figure 5C).

The following explanation can be proposed for the DSC data. The specific 14-3-3ζ_m–pHspB6 complex is stabilized by noncovalent bonds between two proteins; hence, dissociation of this complex is accompanied by disruption of these bonds that will have an endothermic effect. This is reflected in a significant increase of T_m and calorimetric enthalpy (the area) of the 14-3-3ζ_m thermal transition. This effect is observed only in the case of phosphorylated HspB6. Unphosphorylated HspB6 weakly and nonspecifically interacts with 14-3-3ζ_m, and therefore its effect at low temperatures is negligible. Further increase of temperature is accompanied by dissociation of both specific and nonspecific complexes of 14-3-3ζ_m with HspB6. Dissociated 14-3-3ζ_m becomes unfolded and aggregates. Both HspB6 and pHspB6 possess chaperone-like activity and inhibit 14-3-3ζ_m aggregation. Therefore after 14-3-3ζ_m denaturation (above 60 °C) the temperature dependence of light scattering for 14-3-3ζ_m–pHspB6 complex is very similar to that of the mixture of 14-3-3ζ_m with unphosphorylated HspB6 (Figure 6, curves 4 and 5).

Prevention of Myosin S1 Aggregation by 14-3-3ζ. As mentioned earlier, monomeric 14-3-3ζ retains substrate-binding site and is able to interact with certain protein targets with affinity comparable or even higher than the WT dimeric 14-3-3.[23] It is also possible that monomeric 14-3-3 will acquire some new properties because a rather large area buried in the dimer interface becomes exposed upon dimer dissociation.[23] It has been reported that 14-3-3 possesses its own chaperone-like activity and is able to prevent aggregation of partially denatured proteins.[9−12] Therefore, we investigated the ability of different forms of 14-3-3ζ to prevent aggregation of myosin subfragment 1 (S1) as a model substrate which was earlier successfully used for analysis of protein aggregation[44] and chaperone-like activity of HspB1 (Hsp27).[25] Incubation of S1 at the heat shock temperature (43 °C) causes its aggregation, easily detectable by spectroscopic techniques. S1 was incubated at elevated temperature and the effect of 14-3-3ζ_m or dimeric 14-3-3ζ WT on the kinetics of S1 aggregation was monitored by measuring optical density at 360 nm. Both forms of 14-3-3ζ suppressed aggregation and formation of flocculated amorphous aggregates of S1 in a concentration-dependent manner (Figure 7). At all tested weight ratios S1:14-3-3ζ (in the range of 1:0.1−1:1), the 14-3-3 monomer was much more effective than its dimeric counterpart (Figure 7A–D). For instance, at the weight ratio S1/14-3-3ζ equal to 1:1 monomeric 14-3-3 almost completely prevented temperature-induced aggregation of S1, whereas dimeric 14-3-3 only slightly retarded aggregation of S1 (Figure 7D).

We also compared chaperone-like activity of HspB6 and 14-3-3ζ. Under conditions used the dimeric 14-3-3ζ WT and phosphorylated HspB6 possessed roughly equal moderate chaperone-like activity and equally decelerated aggregation of S1 (Figure 7E, curves 2 and 4). At the same time unphosphorylated HspB6 and, especially, monomeric 14-3-3ζ_m possessed a much higher chaperone-like activity and their effect on S1 aggregation was substantially more pronounced (Figure 7E, curves 3 and 5).

DISCUSSION

In the cell 14-3-3 proteins are predominantly present in the form of stable homo- or heterodimers.[4] However, it is reasonable to assume that dimers can be formed only by specific interaction of corresponding monomers which are transiently accumulated in the cell after protein biosynthesis and can participate in subunit exchange. Interestingly, it was shown that specific protein substrates might induce subunit exchange within 14-3-3 dimers leading to formation of selected heterodimers presumably via a substrate-bound monomeric 14-3-3.[45] Recently published data indicate that certain cells can have a splicing isoform of 14-3-3 that is unable to form stable dimers.[19] Moreover, posttranslational modifications (such as phosphorylation of Ser[58]) can induce dissociation of 14-3-3,[15] and therefore certain signals can lead to accumulation of monomers. Thus, under certain conditions the monomeric molecules of 14-3-3 would be present in the cell. However, up to now the structure, properties, and fate of 14-3-3 monomers remain poorly understood. Pilot investigations concerning

dx.doi.org/10.1021/bi300674e | Biochemistry 2012, 51, 6127−6138

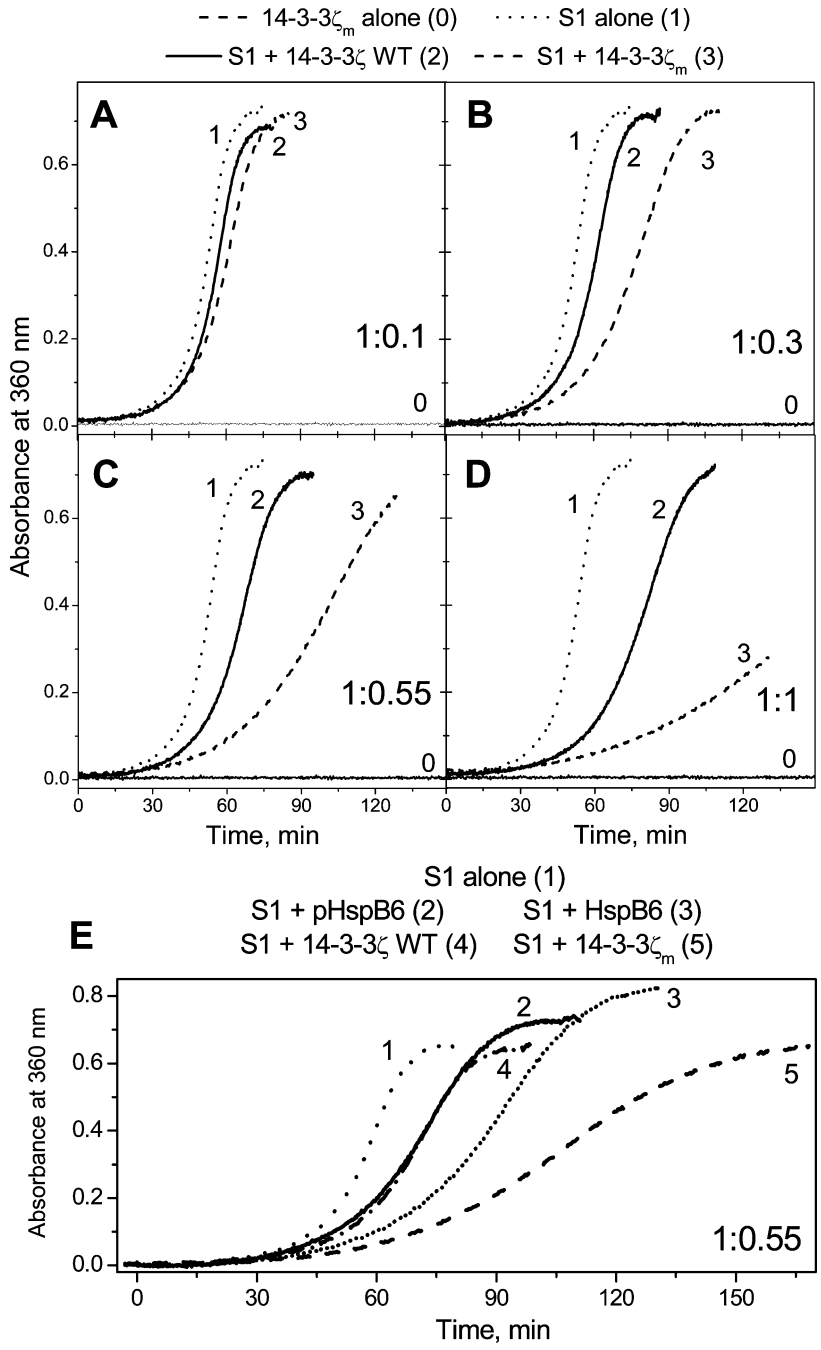

Figure 7. Prevention of the myosin S1 aggregation by 14-3-3ζ_m, 14-3-3ζ WT, and HspB6. S1 aggregation initiated by incubation at the heat shock temperature (43 °C) was monitored by measuring optical density at 360 nm on a Cary 100 UV−visible spectrophotometer. (A−D) Aggregation of S1 alone (0.46 mg/mL; curve 1) or in the presence of 14-3-3ζ WT (curve 2) or 14-3-3ζ_m (curve 3) at different S1/14-3-3 weight ratios which are indicated on each panel. Curve 0 demonstrates that under conditions of the experiment 14-3-3ζ_m (as well as 14-3-3ζ WT and HspB6) does not aggregate. (E) Comparison of the chaperone-like activities of pHspB6 (curve 2), HspB6 (curve 3), 14-3-3ζ WT (curve 4), and 14-3-3ζ_m (curve 5) at a S1/chaperone weight ratio equal to 1:0.55. Curve 1 represents control aggregation of S1.

monomers of 14-3-3[14,17,20,22] were made at a cellular level using extensively mutated proteins with poorly characterized structure. In the previous study, we characterized physicochemical properties of the monomeric form of 14-3-3ζ containing minimal number of mutations.[23] Here, we analyze properties of the monomeric 14-3-3 and investigate the effect of phosphorylated target protein bound to 14-3-3 on its stability.

Earlier, it was shown that the dimeric 14-3-3γ interacts with phosphorylated HspB6 but is unable to form tight complexes with unphosphorylated HspB6 or its phosphomimicking mutant, S16D.[9] Here, by using AF4-MALLS we found that the monomeric 14-3-3ζ also does not interact either with unphosphorylated HspB6 or its phosphomimicking mutant S16D. At the same time the dimer-deficient mutant of 14-3-3 forms stable complexes with the phosphorylated HspB6, with the apparent total molecular mass of 45.0 ± 1.0 kDa. This molecular mass corresponds well with molecular mass expected for a 1:1 complex formed by a monomer of 14-3-3 and monomer of phosphorylated HspB6 (Figure 1 and Figure S1). These data are in good agreement with our earlier results[23] and

dx.doi.org/10.1021/bi300674e | Biochemistry 2012, 51, 6127−6138

indicate that both monomeric and dimeric 14-3-3 tightly interact with phosphorylated HspB6. Formation of this complex is accompanied by dissociation of the usually rather stable dimers of HspB6.

Pseudophosphorylation of HspB6 (Ser16Asp substitution) appears to be insufficient for 14-3-3 binding as only the phosphorylated HspB6 forms stable complexes with monomeric and dimeric 14-3-3. Likewise, the necessity of phosphorylation and an inadequacy of phosphomimicking mutation was previous reported for interaction of 14-3-3 with human keratin 18.[46] On the other hand, Asp/Glu mutant of synaptopodin[47] was able to bind 14-3-3 similarly to phosphorylated protein supporting the suggestion that both the primary structure and environment of phosphorylated Ser/Thr (or Asp and Glu mimicking the site of phosphorylation) are important for recognition of target proteins by 14-3-3.

Interaction of monomeric or dimeric 14-3-3 with pHspB6 might be important for cardioprotective action of HspB6 and its regulation of smooth muscle contraction. Both activities strongly correlate with phosphorylation of HspB6 at Ser^{16} by cyclic nucleotide-dependent protein kinases;[32,48,49] however, the molecular mechanism of these activities remains obscure. We speculate that when present at a relatively high concentration, phosphorylated HspB6 can displace certain enzymes (protein kinases, phosphatases, etc.) or other factors from their complexes with 14-3-3 (discussed in ref 50). It is possible that proteins released during this process participate in cardioprotection and/or regulation of smooth muscle contraction.

Monomeric 14-3-3 is significantly less stable to limited proteolysis than its dimeric counterpart (ref 23 and Figure 2A). This can be due to unmasking of certain sites buried at the subunit interface or due to the overall destabilization of the structure. Addition of phosphorylated HspB6 significantly retarded proteolytic degradation of the monomeric 14-3-3 (Figure 2C) and in the presence of phosphorylated HspB6 the rate of 14-3-3ζ_m degradation became comparable with that of the dimeric 14-3-3 (Figure 2D).

Ser^{16} of HspB6 is the main site effectively phosphorylated by the cyclic-nucleotide dependent protein kinases.[34] Moreover, Ser^{16} is located in the sequence RRApS^{16}APL exactly corresponding to the consensus motif recognized by 14-3-3. Therefore the N-terminal tail of HspB6 appears to be important for interaction with 14-3-3.[32] This region of the small heat shock proteins is very mobile and flexible. This property of the structure can at least partially explain why all attempts to crystallize the full-length human small heat shock proteins were so far unsuccessful. Recently published data provide important information on the structure of α-crystallin domain of small heat shock proteins[33,51] with only preliminary data being available on structure and location of the N-terminal segment.[52] The absence of accurate structural information complicates a detailed analysis of the HspB6 and 14-3-3 interaction. In addition, certain peculiarity of the primary structure of HspB6 hampers accurate identification of peptides responsible for stabilization of the monomeric 14-3-3ζ. However, the limited proteolysis data indicate that even rather short phosphorylated fragments of HspB6 derived from its N-terminal segment make 14-3-3ζ_m more stable to proteolysis. We observed similar stabilization upon addition of inorganic phosphate (Figure 3), that is supposed to occupy phosphopeptide-binding pocket of 14-3-3. The data presented mean that ligand binding stabilizes the structure of 14-3-3ζ_m.

Since binding of phosphorylated HspB6 affected susceptibility of 14-3-3ζ_m to proteolysis, we supposed that formation of the complex can affect the stability of individual proteins. By using different spectroscopic methods we found that addition of phosphorylated HspB6 increased the temperature of 14-3-3ζ_m unfolding, as measured by far-UV CD spectroscopy (Figure 4), and increased half-transition temperature measured by fluorescent spectroscopy (Figure S4, Table 1). Thus, after binding of the phosphorylated HspB6, the 14-3-3ζ_m molecule became more resistant to temperature-induced unfolding.

The stabilizing effect of HspB6 on the 14-3-3ζ_m structure was further analyzed by means of DSC and light scattering (Figures 5 and 6). We found that phosphorylated HspB6 shifted the thermal transition of 14-3-3ζ_m and significantly increased the enthalpy of this transition (Figure 5C, Table 1). This effect appears to be due to multisite specific interactions between the two proteins. In the case of unphosphorylated HspB6, we did not observe such specific interaction, and any effect of HspB6 could be explained by its nonspecific chaperone-like action.

Chaperone-like activity of 14-3-3 was first observed in 1996, when 14-3-3 solubilized ubiquitin-editing zinc finger enzyme A20, altering its cellular localization.[53] Further, it was found that 14-3-3 can act as a conventional chaperone preventing aggregation of protein substrates[9,10] or even by dissolving preformed aggregates.[11] It is thought that 14-3-3 predominantly interacts with proteins containing intrinsically disordered regions.[54] Among these proteins there are many proteins tending to aggregate and 14-3-3 is thought to prevent their aggregation. However, insufficient concentration of 14-3-3 induces aggregation leading to formation of inclusion bodies.[12,13] Chaperone-like activity of 14-3-3 is substrate-dependent: it can either prevent or promote aggregation of analyzed proteins or have no effect.[9,10]

By using subfragment 1 of rabbit skeletal muscle myosin as a model substrate, we found that 14-3-3ζ_m was more effective than the dimeric WT protein in preventing temperature-induced aggregation (Figure 7). Moreover, the chaperone-like effect of 14-3-3ζ_m was no less than that of the unphosphorylated HspB6 and significantly stronger than that of the phosphorylated HspB6 (Figure 7E). The mechanism of chaperone-like action of 14-3-3 remains elusive.[10] However, it is generally supposed that chaperones predominantly recognize and bind misfolded hydrophobic regions on the surface of target proteins. Monomerization of 14-3-3 is accompanied by exposure of a number of hydrophobic residues that are normally buried in the subunit interface (Figure S6),[23] and therefore it is not surprising that 14-3-3ζ_m possesses higher chaperone-like activity than the wild type dimeric 14-3-3ζ. We suggest that in vivo the chaperone action of 14-3-3 might be dependent on the monomeric form of the protein and can be regulated by the monomer/dimer equilibrium.

To summarize, we conclude that the monomeric 14-3-3 retains certain properties of its dimeric counterpart. The monomeric 14-3-3ζ_m is significantly less stable than the dimeric 14-3-3ζ. However, the stability of the 14-3-3ζ_m can be at least partially recovered by its interaction with target proteins. In addition, due to the exposure of residues that are normally buried in the dimer interface, the monomeric 14-3-3 has different properties and possesses higher chaperone-like activity than the dimeric protein.

■ ASSOCIATED CONTENT

Supporting Information

The elution profiles and molecular mass distribution of 14-3-3ζ_m, pHspB6 and their equimolar complex obtained by AF4-MALLS are presented in Figure S1. The secondary structure prediction for HspB6 is shown in Figure S2. Comparison of the fluorescence from tryptophan and HspB6 (or pHspB6) as well as thermally induced fluorescence changes in HspB6 are shown in Figure S3. The effect of pHspB6 on the thermal transition of 14-3-3ζ_m studied by intrinsic tryptophan fluorescence is shown in Figure S4. Differential scanning calorimetry of 14-3-3ζ monomer, 14-3-3ζ dimer, and its phosphomimicking mutants containing S58E substitution is shown in Figure S5. Hydrophobic residues located at the 14-3-3 subunit interface are presented in Figure S6. This material is available free of charge via the Internet at http://pubs.acs.org.

■ AUTHOR INFORMATION

Corresponding Author

*Tel: 7-495-9521384. Fax: 7-495-9542732. E-mail: nikolai.sluchanko@mail.ru.

Funding

This work was supported by grants from Russian Foundation for Basic Research [12-04-31259 to N.N.S., 10-04-00026 to N.B.G. and 12-04-00411 to D.I.L.], by the program "Molecular and Cell Biology" of the Presidium of the Russian Academy of Sciences, and the Wellcome Trust [fellowship 081916 to A.A.A.].

Notes

The authors declare no competing financial interest.

■ ACKNOWLEDGMENTS

We are grateful to Marina V. Serebryakova for her help in MALDI experiments and to Vladimir V. Shubin for his assistance during CD measurements.

■ ABBREVIATIONS USED

14-3-3ζ_m, monomeric mutant form of 14-3-3ζ protein with replacing ^{12}LAE^{14} residues by ^{12}QQR^{14} (earlier named WMW); BSA, bovine serum albumin; DSC, differential scanning calorimetry; DTT, dithiothreitol; ME, β-mercaptoethanol; pHspB6, the small heat shock protein HspB6 (Hsp20) phosphorylated by protein kinase A; PKA and PKG, protein kinases A and G; TLCK, tosyl-L-lysin chloromethyl ketone; WT, wild type

■ REFERENCES

(1) Mackintosh, C. (2004) Dynamic interactions between 14-3-3 proteins and phosphoproteins regulate diverse cellular processes. *Biochem. J. 381*, 329−342.

(2) Yaffe, M. B., Rittinger, K., Volinia, S., Caron, P. R., Aitken, A., Leffers, H., Gamblin, S. J., Smerdon, S. J., and Cantley, L. C. (1997) The structural basis for 14-3-3:phosphopeptide binding specificity. *Cell 91*, 961−971.

(3) Coblitz, B., Wu, M., Shikano, S., and Li, M. (2006) C-terminal binding: an expanded repertoire and function of 14-3-3 proteins. *FEBS Lett. 580*, 1531−1535.

(4) Aitken, A. (2006) 14-3-3 proteins: a historic overview. *Semin. Cancer Biol. 16*, 162−172.

(5) Liu, D., Bienkowska, J., Petosa, C., Collier, R. J., Fu, H., and Liddington, R. (1995) Crystal structure of the zeta isoform of the 14-3-3 protein. *Nature 376*, 191−194.

(6) Yaffe, M. (2002) How do 14-3-3 proteins work?– Gatekeeper phosphorylation and the molecular anvil hypothesis. *FEBS Lett. 513*, 53−57.

(7) Dobson, M., Ramakrishnan, G., Ma, S., Kaplun, L., Balan, V., Fridman, R., and Tzivion, G. (2011) Bimodal regulation of FoxO3 by AKT and 14-3-3. *Biochim. Biophys. Acta 1813*, 1453−1464.

(8) Ganguly, S., Gastel, J. A., Weller, J. L., Schwartz, C., Jaffe, H., Namboodiri, M. A., Coon, S. L., Hickman, A. B., Rollag, M., Obsil, T., Beauverger, P., Ferry, G., Boutin, J. A., and Klein, D. C. (2001) Role of a pineal cAMP-operated arylalkylamine N-acetyltransferase/14-3-3-binding switch in melatonin synthesis. *Proc. Natl. Acad. Sci. U. S. A. 98*, 8083−8088.

(9) Chernik, I., Seit-Nebi, A., Marston, S., and Gusev, N. (2007) Small heat shock protein Hsp20 (HspB6) as a partner of 14-3-3gamma. *Mol. Cell. Biochem. 295*, 9−17.

(10) Williams, D. M., Ecroyd, H., Goodwin, K. L., Dai, H., Fu, H., Woodcock, J. M., Zhang, L., and Carver, J. A. (2011) NMR spectroscopy of 14-3-3zeta reveals a flexible C-terminal extension: differentiation of the chaperone and phosphoserine-binding activities of 14-3-3zeta. *Biochem. J. 437*, 493−503.

(11) Yano, M., Nakamuta, S., Wu, X., Okumura, Y., and Kido, H. (2006) A novel function of 14-3-3 protein: 14-3-3zeta is a heat-shock-related molecular chaperone that dissolves thermal-aggregated proteins. *Mol. Biol. Cell 17*, 4769−4779.

(12) Kaneko, K., and Hachiya, N. (2006) The alternative role of 14-3-3 zeta as a sweeper of misfolded proteins in disease conditions. *Med. Hypotheses 67*, 169−171.

(13) Omi, K., Hachiya, N. S., Tanaka, M., Tokunaga, K., and Kaneko, K. (2008) 14-3-3zeta is indispensable for aggregate formation of polyglutamine-expanded huntingtin protein. *Neurosci. Lett. 431*, 45−50.

(14) Shen, Y., Godlewski, J., Bronisz, A., Zhu, J., Comb, M., Avruch, J., and Tzivion, G. (2003) Significance of 14-3-3 self-dimerization for phosphorylation-dependent target binding. *Mol. Biol. Cell 14*, 4721−4733.

(15) Woodcock, J. M., Murphy, J., Stomski, F. C., Berndt, M. C., and Lopez, A. F. (2003) The dimeric versus monomeric status of 14-3-3zeta is controlled by phosphorylation of Ser58 at the dimer interface. *J. Biol. Chem. 278*, 36323−36327.

(16) Sluchanko, N. N., Chernik, I. S., Seit-Nebi, A. S., Pivovarova, A. V., Levitsky, D. I., and Gusev, N. B. (2008) Effect of mutations mimicking phosphorylation on the structure and properties of human 14-3-3zeta. *Arch. Biochem. Biophys. 477*, 305−312.

(17) Messaritou, G., Grammenoudi, S., and Skoulakis, E. M. (2010) Dimerization is essential for 14-3-3zeta stability and function in vivo. *J. Biol. Chem. 285*, 1692−1700.

(18) Aitken, A. (2011) Post-translational modification of 14-3-3 isoforms and regulation of cellular function. *Semin. Cell Dev. Biol. 22*, 673−680.

(19) Han, D., Ye, G., Liu, T., Chen, C., Yang, X., Wan, B., Pan, Y., and Yu, L. (2010) Functional identification of a novel 14-3-3 epsilon splicing variant suggests dimerization is not necessary for 14-3-3 epsilon to inhibit UV-induced apoptosis. *Biochem. Biophys. Res. Commun. 396*, 401−406.

(20) Tzivion, G., Luo, Z., and Avruch, J. (1998) A dimeric 14-3-3 protein is an essential cofactor for Raf kinase activity. *Nature 394*, 88−92.

(21) Gu, M., and Du, X. (1998) A novel ligand-binding site in the zeta-form 14-3-3 protein recognizing the platelet glycoprotein Ibalpha and distinct from the c-Raf-binding site. *J. Biol. Chem. 273*, 33465−33471.

(22) Zhou, Y., Reddy, S., Murrey, H., Fei, H., and Levitan, I. B. (2003) Monomeric 14-3-3 protein is sufficient to modulate the activity of the Drosophila slowpoke calcium-dependent potassium channel. *J. Biol. Chem. 278*, 10073−10080.

(23) Sluchanko, N. N., Sudnitsyna, M. V., Seit-Nebi, A. S., Antson, A. A., and Gusev, N. B. (2011) Properties of the monomeric form of human 14-3-3zeta protein and its interaction with tau and HspB6. *Biochemistry 50*, 9797−9808.

(24) Bukach, O. V., Seit-Nebi, A. S., Marston, S. B., and Gusev, N. B. (2004) Some properties of human small heat shock protein Hsp20 (HspB6). *Eur. J. Biochem. 271*, 291−302.
(25) Markov, D. I., Pivovarova, A. V., Chernik, I. S., Gusev, N. B., and Levitsky, D. I. (2008) Small heat shock protein Hsp27 protects myosin S1 from heat-induced aggregation, but not from thermal denaturation and ATPase inactivation. *FEBS Lett. 582*, 1407−1412.
(26) Laemmli, U. K. (1970) Cleavage of structural proteins during the assembly of the head of bacteriophage T4. *Nature 227*, 680−685.
(27) Sluchanko, N. N., Sudnitsyna, M. V., Chernik, I. S., Seit-Nebi, A. S., and Gusev, N. B. (2011) Phosphomimicking mutations of human 14-3-3zeta affect its interaction with tau protein and small heat shock protein HspB6. *Arch. Biochem. Biophys. 506*, 24−34.
(28) Rusconi, F. (2009) massXpert 2: a cross-platform software environment for polymer chemistry modelling and simulation/analysis of mass spectrometric data. *Bioinformatics 25*, 2741−2742.
(29) Greenfield, N. J. (2006) Using circular dichroism collected as a function of temperature to determine the thermodynamics of protein unfolding and binding interactions. *Nat. Protoc. 1*, 2527−2535.
(30) Permyakov, E. A., and Burstein, E. A. (1984) Some aspects of studies of thermal transitions in proteins by means of their intrinsic fluorescence. *Biophys. Chem. 19*, 265−271.
(31) Kremneva, E., Nikolaeva, O., Maytum, R., Arutyunyan, A. M., Kleimenov, S. Y., Geeves, M. A., and Levitsky, D. I. (2006) Thermal unfolding of smooth muscle and nonmuscle tropomyosin alpha-homodimers with alternatively spliced exons. *FEBS J. 273*, 588−600.
(32) Dreiza, C. M., Brophy, C. M., Komalavilas, P., Furnish, E. J., Joshi, L., Pallero, M. A., Murphy-Ullrich, J. E., von Rechenberg, M., Ho, Y. S., Richardson, B., Xu, N., Zhen, Y., Peltier, J. M., and Panitch, A. (2005) Transducible heat shock protein 20 (HSP20) phosphopeptide alters cytoskeletal dynamics. *FASEB J. 19*, 261−263.
(33) Baranova, E. V., Weeks, S. D., Beelen, S., Bukach, O. V., Gusev, N. B., and Strelkov, S. V. (2011) Three-dimensional structure of alpha-crystallin domain dimers of human small heat shock proteins HSPB1 and HSPB6. *J. Mol. Biol. 411*, 110−122.
(34) Beall, A., Bagwell, D., Woodrum, D., Stoming, T. A., Kato, K., Suzuki, A., Rasmussen, H., and Brophy, C. M. (1999) The small heat shock-related protein, HSP20, is phosphorylated on serine 16 during cyclic nucleotide-dependent relaxation. *J. Biol. Chem. 274*, 11344−11351.
(35) Bustad, H. J., Underhaug, J., Halskau, O., Jr., and Martinez, A. (2011) The binding of 14-3-3gamma to membranes studied by intrinsic fluorescence spectroscopy. *FEBS Lett. 585*, 1163−1168.
(36) Pozdeyev, N., Taylor, C., Haque, R., Chaurasia, S. S., Visser, A., Thazyeen, A., Du, Y., Fu, H., Weller, J., Klein, D. C., and Iuvone, P. M. (2006) Photic regulation of arylalkylamine N-acetyltransferase binding to 14-3-3 proteins in retinal photoreceptor cells. *J. Neurosci. 26*, 9153−9161.
(37) Pyzhova, N. S., and Nikandrov, V. N. (2008) Effects of biogenic phosphates on protease-induced protein cleavage and functioning of plasminogen activators. *Bioorg. Khim. 34*, 382−391.
(38) Burstein, E. A., Vedenkina, N. S., and Ivkova, M. N. (1973) Fluorescence and the location of tryptophan residues in protein molecules. *Photochem. Photobiol. 18*, 263−279.
(39) Privalov, P. L., and Potekhin, S. A. (1986) Scanning microcalorimetry in studying temperature-induced changes in proteins. *Methods Enzymol. 131*, 4−51.
(40) Brandts, J. F., and Lin, L. N. (1990) Study of strong to ultratight protein interactions using differential scanning calorimetry. *Biochemistry 29*, 6927−6940.
(41) Gesierich, U., and Pfeil, W. (1996) The conformational stability of alpha-crystallin is rather low: calorimetric results. *FEBS Lett. 393*, 151−154.
(42) Kazakov, A. S., Markov, D. I., Gusev, N. B., and Levitsky, D. I. (2009) Thermally induced structural changes of intrinsically disordered small heat shock protein Hsp22. *Biophys. Chem. 145*, 79−85.
(43) Pivovarova, A. V., Mikhailova, V. V., Chernik, I. S., Chebotareva, N. A., Levitsky, D. I., and Gusev, N. B. (2005) Effects of small heat shock proteins on the thermal denaturation and aggregation of F-actin. *Biochem. Biophys. Res. Commun. 331*, 1548−1553.
(44) Markov, D. I., Zubov, E. O., Nikolaeva, O. P., Kurganov, B. I., and Levitsky, D. I. (2010) Thermal denaturation and aggregation of myosin subfragment 1 isoforms with different essential light chains. *Int. J. Mol. Sci. 11*, 4194−4226.
(45) Jagemann, L. R., Perez-Rivas, L. G., Ruiz, E. J., Ranea, J. A., Sanchez-Jimenez, F., Nebreda, A. R., Alba, E., and Lozano, J. (2008) The functional interaction of 14-3-3 proteins with the ERK1/2 scaffold KSR1 occurs in an isoform-specific manner. *J. Biol. Chem. 283*, 17450−17462.
(46) Ku, N. O., Liao, J., and Omary, M. B. (1998) Phosphorylation of human keratin 18 serine 33 regulates binding to 14-3-3 proteins. *EMBO J. 17*, 1892−1906.
(47) Faul, C., Donnelly, M., Merscher-Gomez, S., Chang, Y. H., Franz, S., Delfgaauw, J., Chang, J. M., Choi, H. Y., Campbell, K. N., Kim, K., Reiser, J., and Mundel, P. (2008) The actin cytoskeleton of kidney podocytes is a direct target of the antiproteinuric effect of cyclosporine A. *Nat. Med. 14*, 931−938.
(48) Edwards, H. V., Scott, J. D., and Baillie, G. S. (2012) PKA phosphorylation of the small heat-shock protein Hsp20 enhances its cardioprotective effects. *Biochem. Soc. Trans. 40*, 210−214.
(49) Jerius, H., Karolyi, D. R., Mondy, J. S., Beall, A., Wootton, D., Ku, D., Cable, S., and Brophy, C. M. (1999) Endothelial-dependent vasodilation is associated with increases in the phosphorylation of a small heat shock protein (HSP20). *J. Vasc. Surg. 29*, 678−684.
(50) Sudnitsyna, M. V., Seit-Nebi, A. S., and Gusev, N. B. (2012) Cofilin weakly interacts with 14-3-3 and therefore can only indirectly participate in regulation of cell motility by small heat shock protein HspB6 (Hsp20). *Arch. Biochem. Biophys. 521*, 62−70.
(51) Bagneris, C., Bateman, O. A., Naylor, C. E., Cronin, N., Boelens, W. C., Keep, N. H., and Slingsby, C. (2009) Crystal structures of alpha-crystallin domain dimers of alphaB-crystallin and Hsp20. *J. Mol. Biol. 392*, 1242−1252.
(52) Jehle, S., Vollmar, B. S., Bardiaux, B., Dove, K. K., Rajagopal, P., Gonen, T., Oschkinat, H., and Klevit, R. E. (2011) N-terminal domain of alphaB-crystallin provides a conformational switch for multimerization and structural heterogeneity. *Proc. Natl. Acad. Sci. U. S. A. 108*, 6409−6414.
(53) Vincenz, C., and Dixit, V. M. (1996) 14-3-3 proteins associate with A20 in an isoform-specific manner and function both as chaperone and adapter molecules. *J. Biol. Chem. 271*, 20029−20034.
(54) Bustos, D. M. (2012) The role of protein disorder in the 14-3-3 interaction network. *Mol. Biosyst. 8*, 178−184.